L. Dozio
A Hierarchical Formulation of the State-Space Levy's Method for Vibration Analysis of Thin and Thick Multilayered Shells
Composites Part B - Engineering, Vol. 98, 2016, p. 97-107
doi:10.1016/j.compositesb.2016.05.022

A hierarchical formulation of the state-space Levy's method for vibration analysis of thin and thick multilayered shells

Lorenzo Dozio

Department of Aerospace Science and Technology, Politecnico di Milano, via La Masa, 34, 20156, Milano, Italy

Abstract

The state-space approach in conjunction with the Levy's method is used to solve exactly the free vibration problem of specially orthotropic multilayered cylindrical and spherical panels. A hierarchical formulation is presented to build the matrices of the method from small elementary blocks which are invariant with respect to the order and typology of the kinematic shell theory. As a result, the analytical effort to derive the governing equations is minimized and a large number of Levy-type solution based on low to high order, equivalent single-layer or layerwise theories, can be generated within the same mathematical framework. Thereby, the refinement of the two-dimensional shell model can be tailored according to the thickness ratio and the degree of anisotropy of the problem under study and the desired accuracy. Some illustrative results on both thin and thick, laminated and sandwich panels with various boundary conditions are presented and discussed to show the potential of the formulation.

Keywords: Free vibration, exact solutions, multilayered cylindrical and spherical shells, refined theories, higher-order shell theories, layer-wise shell theories.

1. Introduction

The so-called Levy's method is a well established technique aimed at obtaining exact bending, buckling and vibration solutions of particular plate and shell problems. The origin and name of the method are commonly ascribed to the seminal work of Maurice Levy, who successfully solved in 1899 the bending problem of thin isotropic rectangular plates with simply supported two opposite edges and arbitrary conditions of supports on the two remaining opposite edges using single Fourier series [1]. As observed by Leissa [2], the same type of solution was actually first used by Voigt in 1893 to determine the transverse vibrations of rectangular plates [3]. In spite of this, the single trigonometric series expansion is now conventionally referred to as Levy's solution for both static and dynamic problems [4].

The availability of exact solutions for some plate and shell problems is valuable as they serve as important references for checking the convergence and accuracy of approximate and numerical methods. To this aim,

Email address: lorenzo.dozio@polimi.it (Lorenzo Dozio)

the Levy's method, even if at the cost of greater complexity, is more general and of practical interest than the Navier's method, which is restricted to exact analysis of plates and shells with all edges simply supported. However, it does not have an entirely general character and shares some limitations with the Navier's method, since both can be applied only to particular geometries (i.e., rectangular plates, cylindrical and spherical shells) and material symmetries (i.e., specially orthotropic structures), for which an exact solution of the corresponding boundary-value problem is viable.

This paper is focused on the application of the Levy's method to vibration problems, which has a long and successful history, especially for plates [2, 5, 6, 7, 8, 9, 10, 11, 12, 13, 14, 15, 16, 17, 18, 19, 20, 21, 22, 23, 24]. In particular, the present work is aimed at presenting an advanced state-space formulation of the method for two-dimensional (2-D) exact vibration analysis of cylindrical and spherical single- and multi-layered specially orthotropic panels having both small and large thickness and shallowness ratios. It is worth noting that, contrary to the fairly large number of papers on plates, very few works are available in the open literature on Levy-type vibration solutions of shells [25, 26, 27, 28, 29]. The main novelty of the present contribution relies on a versatile hierarchical technique to build the final matrices of the state-space Levy's method from elementary blocks, called fundamental nuclei, which are invariant with respect to the 2-D kinematic shell theories. In so doing, the tedious and cumbersome analytical effort required for deriving the governing equations related to each specific theory is avoided and a large family of Levy-type vibration solutions of curved panels based on kinematic theories of different order and typology can be automatically generated within the same mathematical framework. The methodology stems from the powerful technique developed by Carrera [30] and makes extensive use of indicial notation. The application of the Carrera's formulation to the Levy's method was originally proposed by the present author for laminated and FGM plates [31, 32] and recently applied by Rezaei and Saidi for vibration analysis of thick porous-cellular plates [33]. In this work, the method is generalized and extended to curved panels.

As shown later, the hierarchical nature of the present formulation allows the accurate exact vibration analysis of both thin and thick, deep and shallow multilayered shell structures. Indeed, an exact 2-D analysis of a multilayered shell does not imply that the corresponding results are also accurate compared to a truly three-dimensional (3-D) analysis. It is known that the thickness ratio (defined as the ratio between the thickness of the panel to the shortest of the span lengths or radii of curvature) and the shallowness ratio (defined as the ratio of the shortest span length to one of the radii of curvature) are two important parameters governing the choice of an appropriate 2-D kinematic model of the curved panel having a desired accuracy [34]. Classical low-order theories are typically employed when the panel is thin and shallow, whereas refined higher-order 2-D shell theories are required to achieve a satisfactory accuracy for thick and deep shells. The accuracy is also largely affected by the frequency range of interest and the degree of anisotropy in the thickness direction [35]. Broadly speaking, for a fixed kinematic theory it usually degrades as the wavelength of the vibration mode is of the order of magnitude of the panel thickness and as the

variation of mechanical properties through the thickness direction increases like the case of sandwich panels. By means of the present formulation, the refinement of the shell model can be tailored on the specific case under investigation and the accuracy of the refined model can benefit from the exactness of the Levy-type solution, without being adversely influenced by the convergence and stability properties of an approximate method.

The paper is organized as follows. After some preliminary definitions in Section 2 and a concise presentation in Section 3 of the family of 2-D shell theories employed in this work, the equations of motion and related boundary conditions of cylindrical and spherical panels are presented in Section 4 according to the compact indicial form introduced by Carrera [30]. The hierarchical construction of the matrices involved in the Levy-type solutions from small invariant elementary blocks is detailed in Section 5. Some illustrative vibration results based on shell theories of different order and typology are shown in Section 6 along with comparison with exact 3-D analysis and other 2-D approaches. Finally, Section 7 contains some concluding remarks.

2. Preliminaries

Let's consider the cylindrical and spherical multilayered panels in Figure 1, which are composed of N_ℓ layers of homogeneous orthotropic material. Each layer k has thickness h_k and is numbered sequentially from bottom ($k = 1$) to top ($k = N_\ell$) of the panel. The total thickness of the panel is $h = \sum_{k=1}^{N_\ell} h_k$. The undeformed middle surface Ω_k of each layer is described by the two orthogonal curvilinear coordinates α and β. Let z_k denote the rectilinear local thickness coordinate in the normal direction with respect to Ω_k. The components of the displacement field $\mathbf{u}^k$ of the k-th layer are indicated as u^k_α, u^k_β and u^k_z in the α, β and z directions, respectively.

According to 3-D elasticity and considering curved panels with constant curvature, the in-plane strains $\boldsymbol{\varepsilon}^k_{\mathrm{p}} = \left\{ \begin{array}{ccc} \varepsilon^k_{\alpha\alpha} & \varepsilon^k_{\beta\beta} & \gamma^k_{\alpha\beta} \end{array} \right\}^{\mathrm{T}}$ of layer k can be expressed as a function of the displacement components $\mathbf{u}^k = \left\{ \begin{array}{ccc} u^k_\alpha & u^k_\beta & u^k_z \end{array} \right\}^{\mathrm{T}}$ by the following relation:

$$\boldsymbol{\varepsilon}^k_{\mathrm{p}} = \left(\boldsymbol{\mathcal{D}}^k_{\mathrm{p}} + \boldsymbol{\mathcal{A}}^k_{\mathrm{p}} \right) \mathbf{u}^k \tag{1}$$

where

$$\boldsymbol{\mathcal{D}}^k_{\mathrm{p}} = \begin{bmatrix} \frac{1}{H^k_\alpha}\frac{\partial}{\partial\alpha} & 0 & 0 \\ 0 & \frac{1}{H^k_\beta}\frac{\partial}{\partial\beta} & 0 \\ \frac{1}{H^k_\beta}\frac{\partial}{\partial\beta} & \frac{1}{H^k_\alpha}\frac{\partial}{\partial\alpha} & 0 \end{bmatrix} \qquad \boldsymbol{\mathcal{A}}^k_{\mathrm{p}} = \begin{bmatrix} 0 & 0 & \frac{1}{H^k_\alpha R^k_\alpha} \\ 0 & 0 & \frac{1}{H^k_\beta R^k_\beta} \\ 0 & 0 & 0 \end{bmatrix} \tag{2}$$

R^k_α and R^k_β are the curvature radii of the α and β coordinate curves, respectively, at the generic point of the middle surface Ω_k of the layer, and

$$H^k_\alpha = 1 + \frac{z_k}{R^k_\alpha} \qquad H^k_\beta = 1 + \frac{z_k}{R^k_\beta} \tag{3}$$

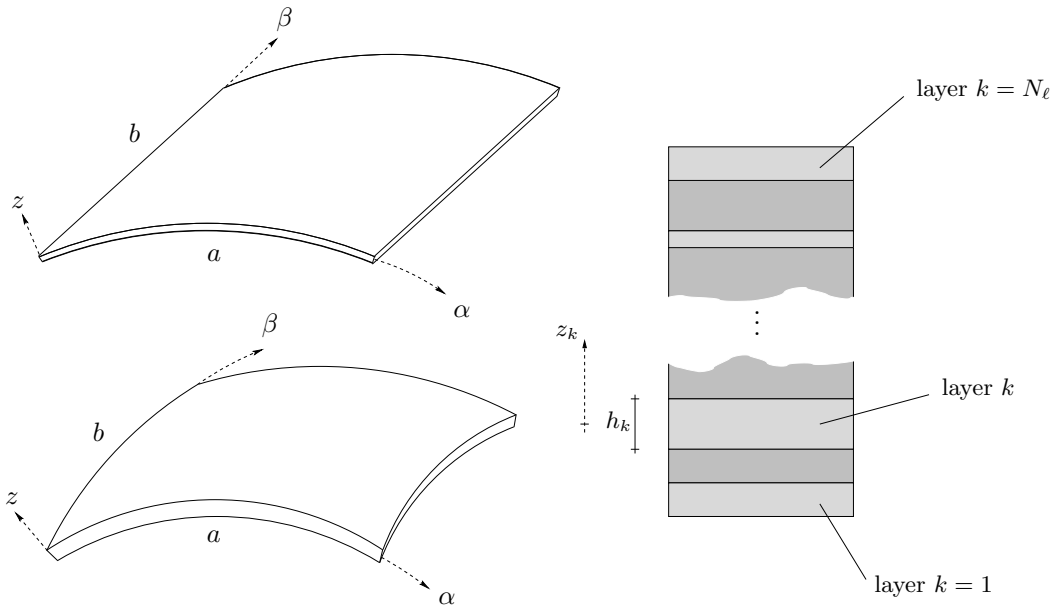

Figure 1: Geometry of the multilayered cylindrical and spherical panels considered in this work and details of the lamination lay-up.

It is noted that $H_\alpha^k = 1$ for cylindrical panels since $R_\alpha^k = \infty$ and $H_\alpha^k = H_\beta^k$ for spherical panels since $R_\alpha^k = R_\beta^k$. Note also that when $1/R_\alpha^k = 1/R_\beta^k = 0$, the above relations degenerate to those for plates.

Similarly, the normal strain components $\boldsymbol{\varepsilon}_{\mathrm{n}}^k = \left\{ \begin{array}{ccc} \gamma_{\alpha z}^k & \gamma_{\beta z}^k & \varepsilon_{zz}^k \end{array} \right\}^{\mathrm{T}}$ can be expressed as follows

$$\boldsymbol{\varepsilon}_{\mathrm{n}}^k = \left(\boldsymbol{\mathcal{D}}_{\mathrm{n}}^k - \boldsymbol{\mathcal{A}}_{\mathrm{n}}^k + \boldsymbol{\mathcal{D}}_z^k \right) \mathbf{u}^k \tag{4}$$

where

$$\boldsymbol{\mathcal{D}}_{\mathrm{n}}^k = \begin{bmatrix} 0 & 0 & \frac{1}{H_\alpha^k}\frac{\partial}{\partial \alpha} \\ 0 & 0 & \frac{1}{H_\beta^k}\frac{\partial}{\partial \beta} \\ 0 & 0 & 0 \end{bmatrix} \qquad \boldsymbol{\mathcal{A}}_{\mathrm{n}}^k = \begin{bmatrix} \frac{1}{H_\alpha^k R_\alpha^k} & 0 & 0 \\ 0 & \frac{1}{H_\beta^k R_\beta^k} & 0 \\ 0 & 0 & 0 \end{bmatrix} \tag{5}$$

and $\boldsymbol{\mathcal{D}}_z^k = \frac{\partial}{\partial z}\mathbf{I}_3$.

Assuming a linearly elastic orthotropic material, the constitutive equations of the k-th layer in the laminate reference coordinate system are written as

$$\begin{aligned} \boldsymbol{\sigma}_{\mathrm{p}}^k &= \tilde{\mathbf{C}}_{\mathrm{pp}}^k \boldsymbol{\varepsilon}_{\mathrm{p}}^k + \tilde{\mathbf{C}}_{\mathrm{pn}}^k \boldsymbol{\varepsilon}_{\mathrm{n}}^k \\ \boldsymbol{\sigma}_{\mathrm{n}}^k &= \tilde{\mathbf{C}}_{\mathrm{pn}}^{k^{\mathrm{T}}} \boldsymbol{\varepsilon}_{\mathrm{p}}^k + \tilde{\mathbf{C}}_{\mathrm{nn}}^k \boldsymbol{\varepsilon}_{\mathrm{n}}^k \end{aligned} \tag{6}$$

where $\boldsymbol{\sigma}_{\mathrm{p}}^k = \left\{ \begin{array}{ccc} \sigma_{\alpha\alpha}^k & \sigma_{\beta\beta}^k & \tau_{\alpha\beta}^k \end{array} \right\}^{\mathrm{T}}$ is the vector of in-plane stresses, $\boldsymbol{\sigma}_{\mathrm{n}}^k = \left\{ \begin{array}{ccc} \tau_{\alpha z}^k & \tau_{\beta z}^k & \sigma_{zz}^k \end{array} \right\}^{\mathrm{T}}$ is the vector

of normal stresses, and the matrices of stiffness coefficients given by

$$\tilde{\mathbf{C}}^k_{\mathrm{pp}} = \begin{bmatrix} \tilde{C}^k_{11} & \tilde{C}^k_{12} & \tilde{C}^k_{16} \\ \tilde{C}^k_{12} & \tilde{C}^k_{22} & \tilde{C}^k_{26} \\ \tilde{C}^k_{16} & \tilde{C}^k_{26} & \tilde{C}^k_{66} \end{bmatrix} \qquad \tilde{\mathbf{C}}^k_{\mathrm{pn}} = \begin{bmatrix} 0 & 0 & \tilde{C}^k_{13} \\ 0 & 0 & \tilde{C}^k_{23} \\ 0 & 0 & \tilde{C}^k_{36} \end{bmatrix} \qquad \tilde{\mathbf{C}}^k_{\mathrm{nn}} = \begin{bmatrix} \tilde{C}^k_{55} & \tilde{C}^k_{45} & 0 \\ \tilde{C}^k_{45} & \tilde{C}^k_{44} & 0 \\ 0 & 0 & \tilde{C}^k_{33} \end{bmatrix} \tag{7}$$

are derived from those expressed in the layer reference system through a proper coordinate transformation [36].

3. 2-D shell theories

By means of the indicial notation introduced by Carrera [30], an entire class of 2-D shell theories can be represented by expanding the displacement vector $\mathbf{u}^k$ in terms of the free parameter j as follows

$$\mathbf{u}^k(\alpha, \beta, \zeta_k, t) = F_j(\zeta_k)\mathbf{u}^k_j(\alpha, \beta, t) \tag{8}$$

where $\zeta_k = 2z_k/h_k$ is the dimensionless thickness coordinate of the layer ($-1 \leq \zeta_k \leq 1$), j is the theory-related index, $F_j(\zeta_k)$ are appropriate thickness functions defined locally for each layer, and $\mathbf{u}^k_j(\alpha, \beta, t) = \left\{ \begin{array}{ccc} u^k_{\alpha j}(\alpha, \beta, t) & u^k_{\beta j}(\alpha, \beta, t) & u^k_{zj}(\alpha, \beta, t) \end{array} \right\}^{\mathrm{T}}$ is the vector of 2-D kinematic coordinates corresponding to index j.

A family of so-called discrete-layer or layerwise (LW) shell theories of variable order N, denoted in the following by the acronym LDN, can be directly obtained from Eq. (8) by assuming $j = t, r, b$ ($r = 2, \ldots, N$) and selecting $F_t(\zeta_k) = \frac{1+\zeta_k}{2}$, $F_r(\zeta_k) = P_r(\zeta_k) - P_{r-2}(\zeta_k)$, $F_b(\zeta_k) = \frac{1-\zeta_k}{2}$ where $P_r(\zeta_k)$ is the Legendre polynomial of r-th order. According to the above choice of the thickness functions, $\mathbf{u}^k_t$ and $\mathbf{u}^k_b$ are the displacement values at the top and bottom surfaces of layer k, so that the continuity at each layer interface is easily enforced by setting $\mathbf{u}^k_t = \mathbf{u}^{k+1}_b$.

Equation (8) can also represents a class of equivalent single-layer (ESL) shell theories by dropping the k index and taking global functions to describe the through-the-thickness deformation. In this work, a simple polynomial representation as a function of the global thickness coordinate z is assumed, i.e., $F_t = 1$, $F_r = z^r (r = 2, \ldots, N)$, $F_b = z$. The related N-order member of the ESL family is indicated by EDN.

Using Eq. (8), the geometric relations and constitutive equations of each layer of the curved panel are written, respectively, as

$$\boldsymbol{\varepsilon}^k_{\mathrm{p}} = \left(\boldsymbol{\mathcal{D}}^k_{\mathrm{p}} + \boldsymbol{\mathcal{A}}^k_{\mathrm{p}} \right) F_j \mathbf{u}^k_j \qquad \boldsymbol{\varepsilon}^k_{\mathrm{n}} = \left(\boldsymbol{\mathcal{D}}^k_{\mathrm{n}} - \boldsymbol{\mathcal{A}}^k_{\mathrm{n}} + \boldsymbol{\mathcal{D}}^k_z \right) F_j \mathbf{u}^k_j \tag{9}$$

and

$$\begin{aligned} \boldsymbol{\sigma}^k_{\mathrm{p}} &= \tilde{\mathbf{C}}^k_{\mathrm{pp}} \left(\boldsymbol{\mathcal{D}}^k_{\mathrm{p}} + \boldsymbol{\mathcal{A}}^k_{\mathrm{p}} \right) F_j \mathbf{u}^k_j + \tilde{\mathbf{C}}^k_{\mathrm{pn}} \left(\boldsymbol{\mathcal{D}}^k_{\mathrm{n}} - \boldsymbol{\mathcal{A}}^k_{\mathrm{n}} + \boldsymbol{\mathcal{D}}^k_z \right) F_j \mathbf{u}^k_j \\ \boldsymbol{\sigma}^k_{\mathrm{n}} &= \tilde{\mathbf{C}}^{k^{\mathrm{T}}}_{\mathrm{pn}} \left(\boldsymbol{\mathcal{D}}^k_{\mathrm{p}} + \boldsymbol{\mathcal{A}}^k_{\mathrm{p}} \right) F_j \mathbf{u}^k_j + \tilde{\mathbf{C}}^k_{\mathrm{nn}} \left(\boldsymbol{\mathcal{D}}^k_{\mathrm{n}} - \boldsymbol{\mathcal{A}}^k_{\mathrm{n}} + \boldsymbol{\mathcal{D}}^k_z \right) F_j \mathbf{u}^k_j \end{aligned} \tag{10}$$

4. Equations of motion and boundary conditions

According to the modeling framework outlined in the previous sections, the dynamic equilibrium of the shell can be expressed in weak form by the principle of virtual displacements as follows

$$\begin{aligned}
&\sum_{k=1}^{N_\ell} \int_{\Omega_k} \delta\mathbf{u}_i^{k\mathrm{T}} \rho^k J_{\alpha\beta}^{kij} \frac{\partial^2 \mathbf{u}_j^k}{\partial t^2} \mathrm{d}\alpha\, \mathrm{d}\beta \\
&+ \sum_{k=1}^{N_\ell} \int_{\Omega_k} \int_{\mathcal{Z}_k} \left[\left(\boldsymbol{\mathcal{D}}_{\mathrm{p}}^k \delta\mathbf{u}_i^k \right)^{\mathrm{T}} \boldsymbol{\sigma}_{\mathrm{p}}^k F_i + \left(\boldsymbol{\mathcal{D}}_{\mathrm{n}}^k \delta\mathbf{u}_i^k \right)^{\mathrm{T}} \boldsymbol{\sigma}_{\mathrm{n}}^k F_i \right] H_\alpha^k H_\beta^k \, \mathrm{d}z\, \mathrm{d}\alpha\, \mathrm{d}\beta \\
&+ \sum_{k=1}^{N_\ell} \int_{\Omega_k} \int_{\mathcal{Z}_k} \left[\delta\mathbf{u}_i^{k\mathrm{T}} \boldsymbol{\mathcal{A}}_{\mathrm{p}}^{k\mathrm{T}} \boldsymbol{\sigma}_{\mathrm{p}}^k F_i - \delta\mathbf{u}_i^{k\mathrm{T}} \boldsymbol{\mathcal{A}}_{\mathrm{n}}^{k\mathrm{T}} \boldsymbol{\sigma}_{\mathrm{n}}^k F_i \right] H_\alpha^k H_\beta^k \, \mathrm{d}z\, \mathrm{d}\alpha\, \mathrm{d}\beta \\
&+ \sum_{k=1}^{N_\ell} \int_{\Omega_k} \int_{\mathcal{Z}_k} \delta\mathbf{u}_i^{k\mathrm{T}} \boldsymbol{\mathcal{D}}_z^{k\mathrm{T}} \boldsymbol{\sigma}_{\mathrm{n}}^k F_i H_\alpha^k H_\beta^k \, \mathrm{d}z\, \mathrm{d}\alpha\, \mathrm{d}\beta = 0
\end{aligned} \tag{11}$$

where $\mathcal{Z}_k$ is the layer domain in the thickness direction and the thickness integral $J_{\alpha\beta}^{kij}$ is defined in the Appendix.

Equation (11) is integrated by parts to relieve the displacement variables by any differentiation and the arbitrariness of each virtual variation is imposed over Ω_k to obtain the following set of equations of motion in indicial notation:

$$\delta\mathbf{u}_i^k : \qquad \rho^k J_{\alpha\beta}^{kij} \frac{\partial^2 \mathbf{u}_j^k}{\partial t^2} + \boldsymbol{\mathcal{L}}^{kij} \mathbf{u}_j^k = \mathbf{0} \tag{12}$$

where $\boldsymbol{\mathcal{L}}^{kij}$ is a 3×3 matrix of differential operators, which can be written using Eq. (10) as

$$\begin{aligned}
\boldsymbol{\mathcal{L}}^{kij} = \int_{\mathcal{Z}_k} \Big\{ &\left(-\boldsymbol{\mathcal{D}}_{\mathrm{p}}^k + \boldsymbol{\mathcal{A}}_{\mathrm{p}}^k \right)^{\mathrm{T}} \tilde{\mathbf{C}}_{\mathrm{pp}}^k \left(\boldsymbol{\mathcal{D}}_{\mathrm{p}}^k + \boldsymbol{\mathcal{A}}_{\mathrm{p}}^k \right) + \left(-\boldsymbol{\mathcal{D}}_{\mathrm{p}}^k + \boldsymbol{\mathcal{A}}_{\mathrm{p}}^k \right)^{\mathrm{T}} \tilde{\mathbf{C}}_{\mathrm{pn}}^k \left(\boldsymbol{\mathcal{D}}_{\mathrm{n}}^k - \boldsymbol{\mathcal{A}}_{\mathrm{n}}^k + \boldsymbol{\mathcal{D}}_z^k \right) \\
&+ \left(-\boldsymbol{\mathcal{D}}_{\mathrm{n}}^k - \boldsymbol{\mathcal{A}}_{\mathrm{n}}^k + \boldsymbol{\mathcal{D}}_z^k \right)^{\mathrm{T}} \tilde{\mathbf{C}}_{\mathrm{pn}}^{k\mathrm{T}} \left(\boldsymbol{\mathcal{D}}_{\mathrm{p}}^k + \boldsymbol{\mathcal{A}}_{\mathrm{p}}^k \right) + \left(-\boldsymbol{\mathcal{D}}_{\mathrm{n}}^k - \boldsymbol{\mathcal{A}}_{\mathrm{n}}^k + \boldsymbol{\mathcal{D}}_z^k \right)^{\mathrm{T}} \tilde{\mathbf{C}}_{\mathrm{nn}}^k \left(\boldsymbol{\mathcal{D}}_{\mathrm{n}}^k - \boldsymbol{\mathcal{A}}_{\mathrm{n}}^k + \boldsymbol{\mathcal{D}}_z^k \right) \Big\} F_i F_j H_\alpha^k H_\beta^k \, \mathrm{d}z
\end{aligned} \tag{13}$$

It is worth noting that Eq. (12) is valid for any index i and the summation for repeated index j is implied. Similarly, the arbitrariness of the virtual variation $\delta\mathbf{u}_i^k$ over the boundary of the panel yields the following set of boundary conditions

$$\boldsymbol{\mathcal{B}}^{kij} \mathbf{u}_j^k = \mathbf{0} \tag{14}$$

where $\boldsymbol{\mathcal{B}}^{kij}$ is another 3×3 matrix of differential operators, which is given for Neumann-type boundary conditions by

$$\begin{aligned}
\boldsymbol{\mathcal{B}}^{kij} = \int_{\mathcal{Z}_k} \Big\{ &\boldsymbol{\mathcal{N}}_{\mathrm{p}}^{k\mathrm{T}} \tilde{\mathbf{C}}_{\mathrm{pp}}^k \left(\boldsymbol{\mathcal{D}}_{\mathrm{p}}^k + \boldsymbol{\mathcal{A}}_{\mathrm{p}}^k \right) + \boldsymbol{\mathcal{N}}_{\mathrm{p}}^{k\mathrm{T}} \tilde{\mathbf{C}}_{\mathrm{pn}}^k \left(\boldsymbol{\mathcal{D}}_{\mathrm{n}}^k - \boldsymbol{\mathcal{A}}_{\mathrm{n}}^k + \boldsymbol{\mathcal{D}}_z^k \right) \\
&+ \boldsymbol{\mathcal{N}}_{\mathrm{n}}^{k\mathrm{T}} \tilde{\mathbf{C}}_{\mathrm{pn}}^{k\mathrm{T}} \left(\boldsymbol{\mathcal{D}}_{\mathrm{p}}^k + \boldsymbol{\mathcal{A}}_{\mathrm{p}}^k \right) + \boldsymbol{\mathcal{N}}_{\mathrm{n}}^{k\mathrm{T}} \tilde{\mathbf{C}}_{\mathrm{nn}}^k \left(\boldsymbol{\mathcal{D}}_{\mathrm{n}}^k - \boldsymbol{\mathcal{A}}_{\mathrm{n}}^k + \boldsymbol{\mathcal{D}}_z^k \right) \Big\} F_i F_j H_\alpha^k H_\beta^k \, \mathrm{d}z
\end{aligned} \tag{15}$$

In the above expression, the matrices $\boldsymbol{\mathcal{N}}^k_{\rm p}$ and $\boldsymbol{\mathcal{N}}^k_{\rm n}$ contains the components n_α and n_β of the unit normal vector to the boundary as follows

$$\boldsymbol{\mathcal{N}}^k_{\rm p} = \begin{bmatrix} \frac{n_\alpha}{H^k_\alpha} & 0 & 0 \\ 0 & \frac{n_\beta}{H^k_\beta} & 0 \\ \frac{n_\beta}{H^k_\beta} & \frac{n_\alpha}{H^k_\alpha} & 0 \end{bmatrix} \qquad \boldsymbol{\mathcal{N}}^k_{\rm n} = \begin{bmatrix} 0 & 0 & \frac{n_\alpha}{H^k_\alpha} \\ 0 & 0 & \frac{n_\beta}{H^k_\beta} \\ 0 & 0 & 0 \end{bmatrix} \tag{16}$$

5. Levy-type solutions for specially orthotropic panels

Exact solutions of the above boundary-value problem are available when the shell panel is at least simply-supported along two opposite edges and is specially orthotropic, i.e., $\tilde{C}^k_{16} = \tilde{C}^k_{26} = \tilde{C}^k_{36} = \tilde{C}^k_{45} = 0$.

Without any loss of generality, let's consider the case where the edges $\beta = 0, b$ of the panel are simply supported. According to the theoretical framework outlined so far, the condition of simple support along $\beta = 0, b$ is specified herein for any index j as follows

$$\begin{aligned} &(\text{along} \quad \beta = 0, b) \\ &\qquad u^k_{\alpha j} = 0 \\ &\qquad \tilde{C}^k_{12} J^{kij} \frac{\partial u^k_{\alpha j}}{\partial \alpha} + \tilde{C}^k_{22} J^{kij}_{\alpha/\beta} \frac{\partial u^k_{\beta j}}{\partial \beta} + \left[\frac{1}{R^k_\alpha} \tilde{C}^k_{12} J^{kij} + \frac{1}{R^k_\beta} \tilde{C}^k_{22} J^{kij}_{\alpha/\beta} + \tilde{C}^k_{23} J^{kij_z}_{\alpha} \right] u^k_{zj} = 0 \\ &\qquad u^k_{zj} = 0 \end{aligned} \tag{17}$$

where the thickness integrals J^{kij}, $J^{kij}_{\alpha/\beta}$ and $J^{kij_z}_{\alpha}$ are given in the Appendix.

A solution for free harmonic motion of the multilayer panel which satisfies the above boundary conditions is sought as follows

$$\mathbf{u}^k_j = \begin{Bmatrix} u^k_{\alpha j} \\ u^k_{\beta j} \\ u^k_{zj} \end{Bmatrix} = \begin{Bmatrix} u^k_{\alpha jn}(\alpha) \sin(\beta_n \beta) \\ u^k_{\beta jn}(\alpha) \cos(\beta_n \beta) \\ u^k_{zjn}(\alpha) \sin(\beta_n \beta) \end{Bmatrix} e^{j\omega t} \qquad (n = 1, 2, \dots) \tag{18}$$

where ω denotes the unknown natural frequency of the shell and $\beta_n = n\pi/b$. Note that the expression in Eq. (18) is indeed a series solution with respect to index n due to the same Einstein notation used before for theory-related indices.

Substituting Eq. (18) into Eq. (12) yields, for each half-wave number n in the β direction, the following system of second-order ordinary differential equations

$$\mathbf{L}^{kij}_2 \frac{\mathrm{d}^2 \mathbf{U}^k_j}{\mathrm{d}\alpha^2} - \mathbf{L}^{kij}_1 \frac{\mathrm{d}\mathbf{U}^k_j}{\mathrm{d}\alpha} - \mathbf{L}^{kij}_0(\omega) \mathbf{U}^k_j = \mathbf{0} \tag{19}$$

where

$$\mathbf{U}^k_j(\alpha) = \begin{Bmatrix} u^k_{\alpha jn}(\alpha) \\ u^k_{\beta jn}(\alpha) \\ u^k_{zjn}(\alpha) \end{Bmatrix} \tag{20}$$

is the vector of unknown amplitudes and

$$\mathbf{L}_2^{kij} = J_{\beta/\alpha}^{kij} \begin{bmatrix} \tilde{C}_{11}^k & 0 & 0 \\ 0 & \tilde{C}_{66}^k & 0 \\ 0 & 0 & \tilde{C}_{55}^k \end{bmatrix} \quad \mathbf{L}_1^{kij} = \begin{bmatrix} 0 & l_{12} & l_{13} \\ l_{21} & 0 & 0 \\ l_{31} & 0 & 0 \end{bmatrix} \quad \mathbf{L}_0^{kij} = \begin{bmatrix} l_{11} & 0 & 0 \\ 0 & l_{22} & l_{23} \\ 0 & l_{32} & l_{33} \end{bmatrix} \tag{21}$$

are 3×3 matrices representing the so-called fundamental nuclei of the governing equations along α direction. As shown later, they are the elementary blocks for the hierarchical generation of the final $\mathbf{L}$ matrices of the method. The elements of $\mathbf{L}_0^{kij}$ and $\mathbf{L}_1^{kij}$ matrices in Eq. (21) are given by

$$\begin{aligned}
l_{11} &= \beta_n^2 \tilde{C}_{66}^k J_{\alpha/\beta}^{kij} + \tilde{C}_{55}^k J_{\alpha\beta}^{ki_z j_z} - \rho^k J_{\alpha\beta}^{kij} \omega^2 + \tilde{C}_{55}^k \left(\frac{1}{{R_\alpha^k}^2} J_{\beta/\alpha}^{kij} - \frac{1}{R_\alpha^k} J_\beta^{ki_z j} - \frac{1}{R_\alpha^k} J_\beta^{kij_z} \right) \\
l_{12} &= \beta_n \left(\tilde{C}_{12}^k + \tilde{C}_{66}^k \right) J^{kij} \\
l_{13} &= \tilde{C}_{55}^k J_\beta^{ki_z j} - \tilde{C}_{13}^k J_\beta^{kij_z} - \tilde{C}_{55}^k \frac{1}{R_\alpha^k} J_{\beta/\alpha}^{kij} - \tilde{C}_{11}^k \frac{1}{R_\alpha^k} J_{\beta/\alpha}^{kij} - \tilde{C}_{12}^k \frac{1}{R_\beta^k} J^{kij} \\
l_{21} &= -\beta_n \left(\tilde{C}_{12}^k + \tilde{C}_{66}^k \right) J^{kij} \\
l_{22} &= \beta_n^2 \tilde{C}_{22}^k J_{\alpha/\beta}^{kij} + \tilde{C}_{44}^k J_{\alpha\beta}^{ki_z j_z} - \rho^k J_{\alpha\beta}^{kij} \omega^2 + \tilde{C}_{44}^k \left(\frac{1}{{R_\beta^k}^2} J_{\alpha/\beta}^{kij} - \frac{1}{R_\beta^k} J_\alpha^{ki_z} - \frac{1}{R_\beta^k} J_\alpha^{kij_z} \right) \\
l_{23} &= \beta_n \left(\tilde{C}_{44}^k J_\alpha^{ki_z j} - \tilde{C}_{23}^k J_\alpha^{kij_z} \right) - \beta_n \left(\tilde{C}_{44}^k \frac{1}{R_\beta^k} J_{\alpha/\beta}^{kij} + \tilde{C}_{12}^k \frac{1}{R_\alpha^k} J^{kij} + \tilde{C}_{22}^k \frac{1}{R_\beta^k} J_{\alpha/\beta}^{kij} \right) \\
l_{31} &= \tilde{C}_{13}^k J_\beta^{ki_z j} - \tilde{C}_{55}^k J_\beta^{kij_z} + \tilde{C}_{55}^k \frac{1}{R_\alpha^k} J_{\beta/\alpha}^{kij} + \tilde{C}_{11}^k \frac{1}{R_\alpha^k} J_{\beta/\alpha}^{kij} + \tilde{C}_{12}^k \frac{1}{R_\beta^k} J^{kij} \\
l_{32} &= \beta_n \left(\tilde{C}_{44}^k J_\alpha^{kij_z} - \tilde{C}_{23}^k J_\alpha^{ki_z j} \right) - \beta_n \left(\tilde{C}_{44}^k \frac{1}{R_\beta^k} J_{\alpha/\beta}^{kij} + \tilde{C}_{12}^k \frac{1}{R_\alpha^k} J^{kij} + \tilde{C}_{22}^k \frac{1}{R_\beta^k} J_{\alpha/\beta}^{kij} \right) \\
l_{33} &= \beta_n^2 \tilde{C}_{44}^k J_{\alpha/\beta}^{kij} + \tilde{C}_{33}^k J_{\alpha\beta}^{ki_z j_z} - \rho^k J_{\alpha\beta}^{kij} \omega^2 + \left[\frac{1}{R_\alpha^k} \left(\tilde{C}_{11}^k \frac{1}{R_\alpha^k} J_{\beta/\alpha}^{kij} + 2\tilde{C}_{12}^k \frac{1}{R_\beta^k} J^{kij} + \tilde{C}_{13}^k J_\beta^{kij_z} + \tilde{C}_{13}^k J_\beta^{ki_z j} \right) \right. \\
&\quad \left. + \frac{1}{R_\beta^k} \left(\tilde{C}_{22}^k \frac{1}{R_\beta^k} J_{\alpha/\beta}^{kij} + \tilde{C}_{23}^k J_\alpha^{kij_z} + \tilde{C}_{23}^k J_\alpha^{ki_z j} \right) \right]
\end{aligned}$$

where the various thickness integrals J are explicitly defined in the Appendix.

Along edges $\alpha = 0, a$ we can have any arbitrary combination of clamped, free and simply supported boundary conditions. They are explicitly expressed for each j-th component as follows

– clamped conditions (C):

$$u_{\alpha j}^k = 0 \qquad u_{\beta j}^k = 0 \qquad u_{zj}^k = 0 \tag{22}$$

– free conditions (F):

$$\begin{aligned}
&\tilde{C}^k_{11}J^{kij}_{\beta/\alpha}\frac{\partial u^k_{\alpha j}}{\partial\alpha}+\tilde{C}^k_{12}J^{kij}\frac{\partial u^k_{\beta j}}{\partial\beta}+\left[\frac{1}{R^k_\alpha}\tilde{C}^k_{11}J^{kij}_{\beta/\alpha}+\frac{1}{R^k_\beta}\tilde{C}^k_{12}J^{kij}+\tilde{C}^k_{13}J^{kij_z}_{\beta}\right]u^k_{zj}=0\\
&\tilde{C}^k_{66}J^{kij}\frac{\partial u^k_{\alpha j}}{\partial\beta}+\tilde{C}^k_{66}J^{kij}_{\beta/\alpha}\frac{\partial u^k_{\beta j}}{\partial\alpha}=0\\
&\left[\tilde{C}^k_{55}J^{kij_z}_{\beta}-\frac{1}{R^k_\alpha}\tilde{C}^k_{55}J^{kij}_{\beta/\alpha}\right]u^k_{\alpha j}+\tilde{C}^k_{55}J^{kij}_{\beta/\alpha}\frac{\partial u^k_{zj}}{\partial\alpha}=0
\end{aligned}\tag{23}$$

– simply-supported conditions (S):

$$\begin{aligned}
&\tilde{C}^k_{11}J^{kij}_{\beta/\alpha}\frac{\partial u^k_{\alpha j}}{\partial\alpha}+\tilde{C}^k_{12}J^{kij}\frac{\partial u^k_{\beta j}}{\partial\beta}+\left[\frac{1}{R^k_\alpha}\tilde{C}^k_{11}J^{kij}_{\beta/\alpha}+\frac{1}{R^k_\beta}\tilde{C}^k_{12}J^{kij}+\tilde{C}^k_{13}J^{kij_z}_{\beta}\right]u^k_{zj}=0\\
&u^k_{\beta j}=0\\
&u^k_{zj}=0
\end{aligned}\tag{24}$$

Substituting Eq. (18) into the above expressions yields, for each $n=1,2,\ldots$, the following equations for each layer k

$$\mathbf{B}^{kij}_1\frac{\mathrm{d}\mathbf{U}^k_j}{\mathrm{d}\alpha}+\mathbf{B}^{kij}_0\mathbf{U}^k_j=\mathbf{0}\qquad\qquad(\alpha=0,a)\tag{25}$$

where $\mathbf{B}^{kij}_0$ and $\mathbf{B}^{kij}_1$ are the 3×3 fundamental nuclei corresponding to the boundary conditions. According to the type of edge condition at $\alpha=0,a$, the boundary-related nuclei are expressed as follows

– clamped edge:

$$\mathbf{B}^{kij}_1=\begin{bmatrix}0&0&0\\0&0&0\\0&0&0\end{bmatrix}\qquad\mathbf{B}^{kij}_0=\begin{bmatrix}\delta_{ij}&0&0\\0&\delta_{ij}&0\\0&0&\delta_{ij}\end{bmatrix}\qquad(\delta_{ij}\text{ is the Kronecker delta})$$

– free edge:

$$\mathbf{B}^{kij}_1=J^{kij}_{\beta/\alpha}\begin{bmatrix}\tilde{C}^k_{11}&0&0\\0&\tilde{C}^k_{66}&0\\0&0&\tilde{C}^k_{55}\end{bmatrix}$$

$$\mathbf{B}^{kij}_0=\begin{bmatrix}0&-\beta_n\tilde{C}^k_{12}J^{kij}&\tilde{C}^k_{13}J^{kij_z}_{\beta}+\frac{1}{R^k_\alpha}\tilde{C}^k_{11}J^{kij}_{\beta/\alpha}+\frac{1}{R^k_\beta}\tilde{C}^k_{12}J^{kij}\\\beta_n\tilde{C}^k_{66}J^{kij}&0&0\\\tilde{C}^k_{55}J^{kij_z}_{\beta}-\frac{1}{R^k_\alpha}\tilde{C}^k_{55}J^{kij}_{\beta/\alpha}&0&0\end{bmatrix}$$

– simply-supported edge:

$$\mathbf{B}^{kij}_1=J^{kij}_{\beta/\alpha}\begin{bmatrix}\tilde{C}^k_{11}&0&0\\0&0&0\\0&0&0\end{bmatrix}\qquad\mathbf{B}^{kij}_0=\begin{bmatrix}0&-\beta_n\tilde{C}^k_{12}J^k_{ij}&\tilde{C}^k_{13}J^{kij_z}_{\beta}+\frac{1}{R^k_\alpha}\tilde{C}^k_{11}J^{kij}_{\beta/\alpha}+\frac{1}{R^k_\beta}\tilde{C}^k_{12}J^{kij}\\0&\delta_{ij}&0\\0&0&\delta_{ij}\end{bmatrix}$$

It is noted that Eqs. (19) and (25) are written in a compact indicial notation for each pair (i, j) and for each layer k of the curved panel in terms of the five fundamental nuclei $\mathbf{L}_2^{kij}$, $\mathbf{L}_1^{kij}$, $\mathbf{L}_0^{kij}$, $\mathbf{B}_1^{kij}$ and $\mathbf{B}_0^{kij}$. The final set of governing equations and boundary conditions for the whole panel corresponding to an ESL or LW kinematic theory of order N can be hierarchically obtained from the previous 3×3 blocks through a simple expansion and assembly-like procedure as explained below.

The first step implies the expansion of the fundamental nuclei by varying the theory-related indices i and j according to the order of the theory. The following square matrices of size $3(N+1)$ are obtained

$$\mathbf{L}^k_{(0,1,2)} = \begin{bmatrix} \mathbf{L}^{ktt}_{(0,1,2)} & \mathbf{L}^{ktr}_{(0,1,2)} & \mathbf{L}^{ktb}_{(0,1,2)} \\ \mathbf{L}^{krt}_{(0,1,2)} & \mathbf{L}^{krr}_{(0,1,2)} & \mathbf{L}^{krb}_{(0,1,2)} \\ \mathbf{L}^{kbt}_{(0,1,2)} & \mathbf{L}^{kbr}_{(0,1,2)} & \mathbf{L}^{kbb}_{(0,1,2)} \end{bmatrix} \qquad \mathbf{B}^k_{(0,1)} = \begin{bmatrix} \mathbf{B}^{ktt}_{(0,1)} & \mathbf{B}^{ktr}_{(0,1)} & \mathbf{B}^{ktb}_{(0,1)} \\ \mathbf{B}^{krt}_{(0,1)} & \mathbf{B}^{krr}_{(0,1)} & \mathbf{B}^{krb}_{(0,1)} \\ \mathbf{B}^{kbt}_{(0,1)} & \mathbf{B}^{kbr}_{(0,1)} & \mathbf{B}^{kbb}_{(0,1)} \end{bmatrix} \qquad (r = 2, \ldots, N) \tag{26}$$

The corresponding equations at layer-level are given by

$$\begin{aligned} &\mathbf{L}_2^k \frac{\mathrm{d}^2 \mathbf{U}^k}{\mathrm{d}\alpha^2} - \mathbf{L}_1^k \frac{\mathrm{d}\mathbf{U}^k}{\mathrm{d}\alpha} - \mathbf{L}_0^k(\omega)\mathbf{U}^k = \mathbf{0} \\ &\mathbf{B}_1^k \frac{\mathrm{d}\mathbf{U}^k}{\mathrm{d}\alpha} + \mathbf{B}_0^k \mathbf{U}^k = \mathbf{0} \qquad\qquad (\alpha = 0, a) \end{aligned} \tag{27}$$

where

$$\mathbf{U}^k(\alpha) = \left\{ \begin{array}{c} \mathbf{U}^k_t(\alpha) \\ \mathbf{U}^k_r(\alpha) \\ \mathbf{U}^k_b(\alpha) \end{array} \right\} \tag{28}$$

The final multilayer matrices $\mathbf{L}$ and $\mathbf{B}$ are obtained, in case of EDN theories, by simply summing the above layer-level matrices or, in case of LDN theories, by a global assembly procedure along the thickness direction of the panel as a diagonal concatenation of $\mathbf{L}^k_{(0,1,2)}$ and $\mathbf{B}^k_{(0,1)}$ through the imposition of the interlaminar displacement continuity condition [31]. The resulting set of governing equations and boundary conditions is written as

$$\begin{aligned} &\mathbf{L}_2 \frac{\mathrm{d}^2 \mathbf{U}}{\mathrm{d}\alpha^2} - \mathbf{L}_1 \frac{\mathrm{d}\mathbf{U}}{\mathrm{d}\alpha} - \mathbf{L}_0(\omega)\mathbf{U} = \mathbf{0} \\ &\mathbf{B}_1 \frac{\mathrm{d}\mathbf{U}}{\mathrm{d}\alpha} + \mathbf{B}_0 \mathbf{U} = \mathbf{0} \qquad\qquad (\alpha = 0, a) \end{aligned} \tag{29}$$

where $\mathbf{U}(\alpha)$ is the vector containing all the independent kinematic variables $\mathbf{U}^k(\alpha)$ $(k = 1, \ldots, N_\ell)$.

A state-space approach is used to solve the free vibration problem by converting Eqs. (29) into a first-order form as follows

$$\begin{aligned} &\frac{\mathrm{d}\mathbf{Z}}{\mathrm{d}\alpha} = \mathbf{A}\mathbf{Z} \\ &\mathbf{B}\mathbf{Z} = \mathbf{0} \qquad\qquad (\alpha = 0, a) \end{aligned} \tag{30}$$

where

$$\mathbf{Z}(\alpha) = \left\{ \begin{array}{c} \mathrm{d}\mathbf{U}/\mathrm{d}\alpha \\ \mathbf{U} \end{array} \right\} \tag{31}$$

and

$$\mathbf{A} = \begin{bmatrix} \mathbf{L}_2 & \mathbf{0} \\ \mathbf{0} & \mathbf{I} \end{bmatrix}^{-1} \begin{bmatrix} \mathbf{L}_1 & \mathbf{L}_0 \\ \mathbf{I} & \mathbf{0} \end{bmatrix}, \qquad \mathbf{B} = \begin{bmatrix} \mathbf{B}_1 & \mathbf{B}_0 \end{bmatrix} \tag{32}$$

The general solution of Eq. (30) can be expressed in terms of the matrix exponential of $\mathbf{A}$ as

$$\mathbf{Z}(\alpha) = e^{\mathbf{A}\alpha}\mathbf{c} \tag{33}$$

where $\mathbf{c}$ is a vector of constants connected to boundary conditions. Using a spectral decomposition of the exponential matrix, the solution is given by

$$\mathbf{Z}(\alpha) = \mathbf{V}\text{Diag}\left(e^{\lambda_i \alpha}\right)\mathbf{V}^{-1}\mathbf{c} \tag{34}$$

where $\mathbf{V}$ is the matrix of eigenvectors of $\mathbf{A}$ and λ_i are the corresponding eigenvalues. Replacement of solution (34) into the system of boundary equations in Eq. (30) yields a homogeneous system

$$\mathbf{H}\mathbf{c} = \mathbf{0} \qquad (\alpha = 0, a) \tag{35}$$

where $\mathbf{H} = \mathbf{B}\mathbf{V}\text{Diag}\left(e^{\lambda_i \alpha}\right)\mathbf{V}^{-1}$. The natural frequencies associated with the imposed half-wave number n are determined by setting $\det(\mathbf{H}) = 0$. Note that, since $\mathbf{H} = \mathbf{H}(\omega)$, a simple iterative numerical procedure is employed to derive the frequency parameters by checking when the determinant of $\mathbf{H}$ changes sign and using a bisection method around the guess zero value to refine the solution.

6. Results

6.1. Example 1

The first example involves a fully simply-supported single-layer orthotropic spherical shell panel, with radii of curvature $R_\alpha = R_\beta = 10$ m, and dimensions $a = b = (\pi/3)R_\alpha$. The orthotropic layer has the following material properties: $E_1 = 132.38$ GPa, $E_2 = E_3 = 10.756$ GPa, $G_{12} = G_{13} = 5.6537$ GPa, $G_{23} = 3.603$ GPa, $\nu_{12} = \nu_{13} = 0.24$, $\nu_{23} = 0.49$, and mass density $\rho = 1600$ kg/m^3. Table 1 presents six non-dimensional frequency parameters $\hat{\omega} = \omega(a^2/h)\sqrt{\rho/E_2}$ when the half-wave number n in the β direction is imposed to be equal to 1 and 2. Results corresponding to various thickness ratios h/R_α are shown for equivalent single-layer theories of increasing order ($N = 2, 3, 4$) and are all automatically computed from the same computer code by exploiting the hierarchical nature of the present formulation. Present 2-D exact values are compared with 3-D exact analysis provided by Brischetto [37]. It is observed that, as expected, when the panel is thin ($h/R_\alpha = 0.001$ and 0.01), all theories give the same theoretical predictions and increasing the order of the 2-D model does not provide any substantial improvement. For moderately thick panels ($h/R_\alpha = 0.1$), accurate frequency parameters are obtained for $N \geq 3$, especially when higher-order modes are evaluated. When a thicker shell is considered, this effect is amplified, and values close to 3-D

results in the entire frequency range of interest are achieved only with a fourth-order theory. Figure 2 shows that the local through-the-thickness distribution of displacements corresponding to three vibration modes when $h/R_\alpha = 0.2$ is also well captured by an ED4 model. Comparison with 3-D profiles is given in terms of normalized modal values $\hat{u} = u/|u_{\max}|$, $\hat{v} = v/|v_{\max}|$, and $\hat{w} = w/|w_{\max}|$ evaluated at $(\alpha, \beta) = (0, b/2)$, $(\alpha, \beta) = (a/2, 0)$ and $(\alpha, \beta) = (a/2, b/2)$, respectively. It is worth noting the non-linear deformed pattern of the in-plane modal displacements and the non-constant profile of the out-of-plane component, which are due to the relatively large thickness ratio of the panel. Both effects are magnified for high-frequency modes.

Table 1: Example 1. Dimensionless frequencies $\hat{\omega} = \omega(a^2/h)\sqrt{\rho/E_2}$ of a simply-supported single-layer orthotropic spherical panel when $n = 1$ and $n = 2$. Comparison among 3-D exact analysis and EDN ($N = 2, 3, 4$) models for various thickness ratios h/R_α.

h/R_α		Model					Model			
		3D-exact [37]	ED2	ED3	ED4		3D-exact [37]	ED2	ED3	ED4
0.001	$n = 1$	1114.0	1114.0	1114.0	1114.0	$n = 2$	1260.9	1260.9	1260.9	1260.9
		1209.7	1209.7	1209.7	1209.7		1682.9	1682.9	1682.9	1682.9
		4016.5	4016.4	4016.4	4016.4		6838.7	6838.7	6838.7	6838.7
		5758.3	5758.3	5758.3	5758.3		8009.4	8009.4	8009.4	8009.4
		12456	12456	12456	12456		13147	13147	13147	13147
		23599	23599	23599	23599		23985	23985	23985	23985
0.01	$n = 1$	117.90	117.91	117.90	117.90	$n = 2$	133.19	133.20	133.19	133.19
		121.32	121.33	121.33	121.33		169.01	169.00	169.00	169.00
		401.63	401.63	401.63	401.63		683.84	683.84	683.84	683.84
		575.82	575.82	575.82	575.82		800.89	800.90	800.90	800.90
		1245.5	1245.5	1245.5	1245.5		1314.6	1314.6	1314.6	1314.6
		2359.8	2359.8	2359.8	2359.8		2398.3	2398.3	2398.3	2398.3
0.1	$n = 1$	14.754	14.821	14.754	14.754	$n = 2$	21.986	22.089	21.987	21.986
		30.685	31.648	30.693	30.687		34.372	35.336	34.383	34.374
		40.041	40.041	40.041	40.041		68.035	68.041	68.035	68.035
		57.401	57.403	57.401	57.401		79.625	79.634	79.625	79.625
		123.88	123.90	123.88	123.88		130.57	130.60	130.57	130.57
		208.50	216.21	208.60	208.56		216.62	222.99	216.82	216.68
0.2	$n = 1$	9.1755	9.3492	9.1795	9.1761	$n = 2$	14.305	14.552	14.316	14.306
		19.645	19.824	19.688	19.666		22.411	23.345	22.463	22.431
		19.819	20.622	19.819	19.819		33.373	33.418	33.373	33.373
		28.398	28.413	28.401	28.398		39.004	39.077	39.012	39.004
		54.506	57.966	54.555	54.521		60.847	62.897	60.957	60.862
		58.572	58.877	58.625	58.588		65.349	66.248	65.537	65.374

6.2. Example 2

The second example deals with a fully simply-supported three-layered sandwich cylindrical panel. The radius of curvature is taken as $R_\alpha = 10$ m, and the dimensions of the shell are $a = (\pi/3)R_\alpha$ and $b = 20$ m. The sandwich configuration has the skins in aluminum ($E = 73$ GPa, $\nu = 0.3$ and $\rho = 2800$ kg/m^3) with

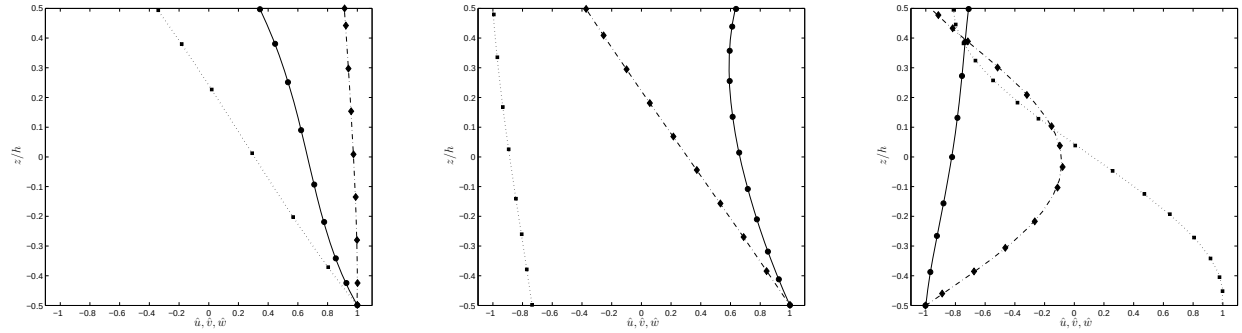

(a) $\hat{\omega} = 9.1761$ (b) $\hat{\omega} = 19.819$ (c) $\hat{\omega} = 54.521$

Figure 2: Example 1 with $h/R_\alpha = 0.2$ and $n = 1$. Through-the-thickness distribution of three vibration modes in terms of displacement components. Comparison between ED4 model and 3-D analysis: $\hat{u} = u/|u_{\max}|$ — present, • 3-D; $\hat{v} = v/|v_{\max}|$ $\cdots$ present, ■ 3-D; $\hat{w} = w/|w_{\max}|$ $-\cdot$ present, ♦ 3-D.

thickness $h_s = 0.2h$ and a foam core in PVC ($E = 180$ MPa, $\nu = 0.37$ and $\rho = 50$ kg/m^3) with thickness $h_c = 0.6h$. The first ten frequencies in Hz corresponding to three different thickness ratios $h/R_\alpha = 0.001$, 0.01, and 0.1 are reported in Table 2 and compared with 3-D exact values available from Ref. [35] (see also Ref. [38] for further details about the 3-D exact solution). For each imposed half-wave number n along β direction, the corresponding half-wave number m in the α direction is identified from the visualization of the vibration modes. In addition to EDN models of increasing order, in this example involving a multilayered structure the frequency values are also computed using LDN theories with N ranging from 1 to 4. In doing so, the accuracy of both approaches can be evaluated in terms of the degree of anisotropy in the thickness direction. From Table 2 it can be observed that, in the case of very thin panels ($h/R_\alpha = 0.001$), higher-order theories or discrete-layer models are useless in practice since accurate predictions can be obtained even with an ED2 model. The situation significantly changes when $h/R_\alpha = 0.01$. Although the panel can be still considered as geometrically thin, equivalent single-layer models introduce large errors in the estimation of natural frequencies. The discrepancy with 3-D analysis dramatically increases as the wave numbers increase and completely unreliable results are computed for higher-order modes. Note also that the accuracy of ED models is not even improved by increasing the order of the theory. This is due to the strong difference in the elastic and mass properties between the foam core and the metallic skins, which calls for a layerwise modeling of the sandwich panel under study. Indeed, values computed from LD1 theory are close to 3-D values for both low and higher vibration modes. The accuracy is only slightly better when second-order layerwise models are assumed. The final case of moderately thick panel ($h/R_\alpha = 0.1$) amplifies what already observed for thin shells. However, a linear discrete-layer model is now rather inadequate in representing the dynamic deformation of the structure and refined LDN theories with $N \geq 2$ are required. Note also that increasing further the order N is unnecessary to improve the estimation of the natural frequencies.

This conclusion is not valid if an accurate representation of the local through-the-thickness distribution of displacement is required, as shown in Figure 3 for the normalized modal displacement $\hat{v}$ corresponding to modes $(2,2)$ and $(2,3)$.

Table 2: Example 2. First ten frequencies (Hz) of simply-supported three-layered sandwich cylindrical panels with h/R_α = 0.001, 0.01, and 0.1. Comparison among 3-D exact analysis and various 2-D shell models.

h/R_α	Mode (m,n)	3D-exact [35]	ED2	ED3	ED4	LD1	LD2	LD3	LD4
0.001	(3,1)	3.644	3.650	3.650	3.650	3.650	3.644	3.644	3.644
	(4,1)	5.082	5.108	5.106	5.106	5.094	5.082	5.082	5.082
	(2,1)	5.230	5.231	5.231	5.231	5.231	5.231	5.229	5.229
	(4,2)	7.269	7.290	7.288	7.288	7.278	7.270	7.270	7.270
	(5,1)	7.667	7.728	7.726	7.726	7.686	7.666	7.666	7.666
	(5,2)	8.554	8.615	8.613	8.613	8.574	8.554	8.554	8.554
	(3,2)	9.179	9.182	9.182	9.182	9.182	9.180	9.180	9.180
	(6,1)	10.93	11.02	11.02	11.02	10.96	10.93	10.93	10.93
	(5,3)	10.97	11.06	11.06	11.06	10.98	10.97	10.97	10.97
	(6,2)	11.41	11.54	11.54	11.54	11.44	11.41	11.41	11.41
0.01	(2,1)	12.19	13.51	13.46	13.46	12.23	12.20	12.20	12.20
	(1,1)	16.62	16.65	16.65	16.65	16.63	16.63	16.63	16.63
	(2,2)	21.41	22.66	22.61	22.61	21.45	21.43	21.43	21.43
	(3,1)	22.17	27.87	27.61	27.61	22.26	22.18	22.18	22.18
	(3,2)	25.16	31.44	31.15	31.15	25.25	25.17	25.17	25.17
	(3,3)	31.30	35.79	35.72	35.72	31.41	31.32	31.32	31.32
	(2,3)	34.27	38.40	38.05	38.05	34.31	34.29	34.29	34.29
	(4,1)	34.58	49.06	48.28	48.28	34.74	34.58	34.58	34.58
	(4,2)	36.21	40.92	40.92	40.92	36.39	36.22	36.22	36.22
	(4,3)	39.44	56.63	55.65	55.65	39.63	39.45	39.45	39.45
0.1	(1,1)	20.04	36.03	33.11	33.11	20.20	20.07	20.07	20.07
	(2,1)	29.48	78.27	78.27	78.27	30.66	29.42	29.42	29.42
	(2,2)	37.10	68.29	62.03	62.01	38.47	37.06	37.06	37.06
	(1,2)	43.94	134.18	101.4	101.2	44.17	43.99	43.99	43.99
	(2,3)	49.74	108.0	92.84	92.79	51.44	49.73	49.72	49.72
	(3,1)	52.80	113.6	87.73	87.63	56.00	52.64	52.62	52.62
	(3,2)	57.02	156.5	156.5	156.5	60.56	56.88	56.86	56.86
	(1,3)	61.47	168.0	123.2	123.0	61.90	61.51	61.51	61.51
	(2,4)	63.85	155.1	123.7	123.6	66.13	63.86	63.85	63.85
	(3,3)	64.73	234.8	179.9	179.2	68.79	64.61	64.58	64.58

6.3. Example 3

The present example refers to a moderately thick cross-ply [0/90/0] laminated panel having the following non-dimensional material properties: $E_1 = 25E_2$, $E_3 = E_2$, $G_{12} = G_{13} = 0.5E_2$, $G_{23} = 0.2E_2$, $\nu_{12} = \nu_{13} = \nu_{23} = 0.25$, $\rho = 1$. Both spherical and cylindrical geometries are analyzed with $a = b$, thickness ratio $h/a = 0.1$ and shallowness ratio $a/R_\alpha = 1/20$. Results are listed in Table 3 for various clamped, free and simply-supported boundary conditions along edges $\alpha = 0, a$ in terms of the fundamental frequency

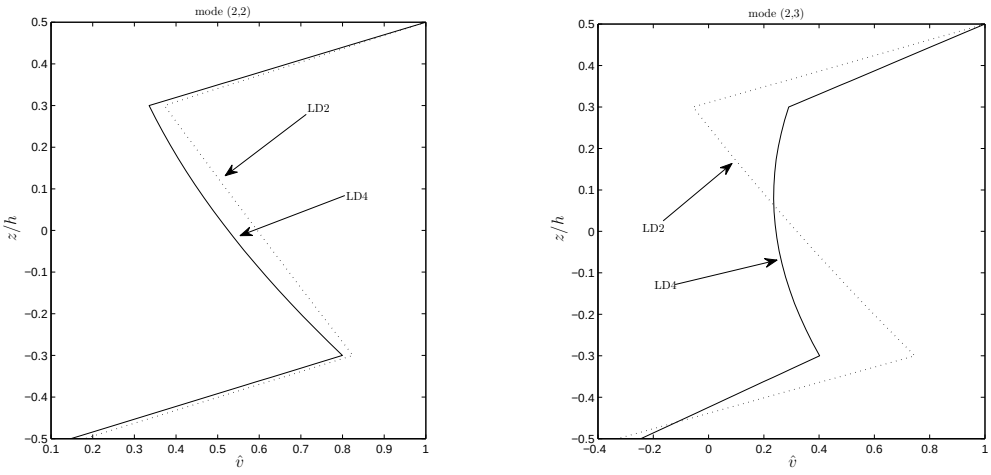

(a) mode (2,2) - $f = 37.06$ Hz (b) mode (2,3) - $f = 49.72$ Hz

Figure 3: Example 2 with $h/R_\alpha = 0.1$. Through-the-thickness distribution of the normalized in-plane displacement $\hat{v} = v/|v_{\max}|$ for vibration modes (2,2) and (2,3). Comparison between LD2 and LD4 solutions.

$\hat{\omega} = \omega(a^2/h)\sqrt{\rho/E_2}$. Present computations come from 2-D equivalent single-layer and layerwise models of different orders and are compared with the exact values obtained by Khdeir and Reddy [25] using the Levy's method based on a third-order shear deformation theory. Some observations can be made from Table 3. First, the large differences between EDN and LDN models previously outlined for moderately thick sandwich panels (see Example 2) are now significantly mitigated since the variation of elastic properties among layers is limited, even though the constituent material has a high degree of orthotropicity. As a result, refined equivalent single-layer models can be considered in most cases as a fairly accurate representation of the fundamental vibrating mode of the panel under study. This conclusion is particularly true when one or two edges are free, as also observed by the good agreement with frequency values available from Ref. [25]. Instead, when the panel has two edges clamped, the fundamental frequency computed using discrete-layer models is remarkably lower than predictions based on ESL theories and very accurate estimations can be obtained only using a layerwise description. As a final remark, it is noted that frequency results corresponding to LD4 models are essentially equal to those of LD3 models.

6.4. Example 4

The last example is aimed at providing some reference exact results for cylindrical and spherical sandwich panels with various boundary conditions. The sandwich configuration is the same as the case of Example 2 for both geometries, i.e., PVC core of thickness $0.6h$ and two aluminum skins each of thickness $0.2h$. The cylindrical panels have radius of curvature $R_\alpha = 10$ m and dimensions $a = (\pi/3)R_\alpha$ and $b = 20$ m. The spherical panels have radii of curvature $R_\alpha = R_\beta = 10$ m and dimensions $a = b = (\pi/3)R_\alpha$. Levy-type solutions are listed in Tables 4 and 5 for thickness ratios $h/R_\alpha = 0.01$ and 0.1, thus encompassing

Table 3: Example 3. Fundamental frequency $\hat{\omega} = \omega(a^2/h)\sqrt{\rho/E_2}$ of laminated [0/90/0] spherical and cylindrical panels with $h/a = 0.1$ and $a/R_\alpha = 1/20$. Comparison of different exact 2-D models for various boundary conditions along edges $\alpha = 0, a$.

	SS	CS	FF	CC	FS	FC
Spherical panel						
Khdeir and Reddy [25]	11.807	13.481	3.797	16.100	4.328	6.088
ED3	11.769	13.684	3.798	15.809	4.331	6.072
ED4	11.769	13.683	3.798	15.806	4.331	6.072
LD1	11.594	13.459	3.812	15.566	4.343	6.043
LD2	11.478	13.293	3.799	15.361	4.329	6.011
LD3	11.472	13.259	3.792	15.296	4.323	6.003
LD4	11.472	13.259	3.792	15.294	4.323	6.003
Cylindrical panel						
Khdeir and Reddy [25]	11.793	13.825	3.789	15.999	4.322	6.089
ED3	11.757	13.674	3.799	15.807	4.333	6.078
ED4	11.757	13.672	3.799	15.803	4.332	6.078
LD1	11.581	13.448	3.813	15.562	4.346	6.049
LD2	11.466	13.282	3.802	15.357	4.331	6.017
LD3	11.458	13.248	3.793	15.292	4.324	6.008
LD4	11.458	13.248	3.793	15.291	4.324	6.008

geometrically thin and moderately thick shells, and different combinations of boundary conditions along edges $\alpha = 0, a$. For benchmarking purposes, present results corresponding to the first ten vibration modes are computed using LD3 models, which have been proved to provide accurate frequency values.

Table 4: Example 4 - Benchmark 1. First ten exact frequencies (Hz) of three-layered sandwich cylindrical panels with $h/R_\alpha = 0.01$ and 0.1, and various boundary conditions. Results are computed using third-order layerwise models.

h/R_α	BCs	Mode									
		1	2	3	4	5	6	7	8	9	10
0.01	CS	13.75	22.62	23.65	29.10	32.33	32.87	37.82	38.09	39.73	41.01
	CC	21.41	24.09	29.17	31.75	36.99	38.79	39.07	45.31	45.49	45.66
	FF	3.101	5.567	9.097	9.407	9.978	14.62	15.34	17.36	20.91	21.37
	FS	4.324	9.312	12.22	14.52	14.98	20.76	21.13	25.74	27.69	28.15
	FC	4.483	9.383	14.06	14.98	21.14	23.07	23.22	27.69	29.78	30.32
0.1	CS	27.90	39.09	39.75	53.13	55.26	59.03	65.31	66.76	68.02	75.50
	CC	39.37	50.63	55.77	60.26	63.15	67.63	74.95	76.62	83.24	84.47
	FF	8.687	10.21	19.54	23.06	26.19	30.30	33.10	36.41	42.31	43.69
	FS	10.49	20.23	21.23	31.56	37.17	38.83	42.95	42.98	53.08	55.65
	FC	12.27	21.39	26.53	31.67	42.65	43.02	43.03	55.67	55.82	55.95

Table 5: Example 4 - Benchmark 2. First ten exact frequencies (Hz) of three-layered sandwich spherical panels with $h/R_\alpha = 0.01$ and 0.1, and various boundary conditions. Results are computed using third-order layerwise models.

h/R_α	BCs	Mode									
		1	2	3	4	5	6	7	8	9	10
0.01	CS	78.32	80.31	81.76	82.99	83.14	85.61	85.62	86.90	87.55	89.51
	CC	81.22	81.33	83.21	83.56	84.74	86.71	87.76	89.30	90.61	90.63
	FF	3.518	4.419	14.06	14.39	27.38	27.43	79.03	80.60	81.65	83.43
	FS	3.934	14.22	27.41	41.65	56.17	70.69	77.91	80.13	80.72	82.45
	FC	7.079	14.22	27.41	41.65	56.17	70.69	79.74	80.91	82.73	84.49
0.1	CS	80.94	86.07	88.82	94.60	97.38	101.4	107.1	109.7	117.8	123.6
	CC	87.78	87.86	90.77	97.74	98.18	108.3	109.5	114.6	118.3	128.7
	FF	12.41	15.93	34.99	35.99	61.60	61.82	83.40	88.54	92.68	93.58
	FS	14.11	35.48	61.71	80.37	86.25	88.63	93.67	95.62	98.01	102.8
	FC	15.48	35.48	61.71	84.31	88.16	92.02	93.67	99.03	99.11	107.7

7. Conclusions

An advanced formulation of the state-space Levy's method is presented for free vibration analysis of isotropic, laminated and sandwich shells. The final matrices of the method are hierarchically obtained from elementary blocks with invariance property towards the order and typology of the shell theory. As a result, exact Levy-type vibration solutions can be obtained from a large variety of 2-D kinematic models, which can be arbitrarily refined according to the accuracy required by the thickness ratio and the degree of through-thickness anisotropy of the problem under study. Some examples for both cylindrical and spherical panels with different combinations of boundary conditions are presented and discussed to demonstrate the potential of the proposed technique. It is shown that the accuracy of an exact 2-D analysis is strongly dependent on the refinement of the 2-D shell theory, in particular when the panel is thick and exhibits strong differences in the elastic and mass properties of its constituent layers. A comprehensive set of new frequency results for both thin and thick sandwich cylindrical and spherical panels is also provided, which can be used as a valuable benchmark for validating approximate numerical methods.

Appendix

The thickness integrals in the fundamental nuclei of the present formulation are defined as follows:

$$\left(J^{kij}, J^{kij}_{\alpha/\beta}, J^{kij}_{\beta/\alpha}, J^{kij}_{\alpha\beta}\right) = \int_{z_k} F_i F_j \left(1, \frac{H^k_\alpha}{H^k_\beta}, \frac{H^k_\beta}{H^k_\alpha}, H^k_\alpha H^k_\beta\right) \mathrm{d}z$$

$$\left(J^{ki_z j}_{\alpha}, J^{ki_z j}_{\beta}\right) = \int_{z_k} \frac{\partial F_i}{\partial z} F_j \left(H^k_\alpha, H^k_\beta\right) \mathrm{d}z$$

$$\left(J^{kij_z}_{\alpha}, J^{kij_z}_{\beta}\right) = \int_{z_k} F_i \frac{\partial F_j}{\partial z} \left(H^k_\alpha, H^k_\beta\right) \mathrm{d}z$$

$$J_{\alpha\beta}^{ki_z j_z} = \int_{Z_k} \frac{\partial F_i}{\partial z} \frac{\partial F_j}{\partial z} H_\alpha^k H_\beta^k \mathrm{d}z$$

References

[1] M. Levy, Memoire sur la theorie des plaques elastiques planes, *Journal de mathématiques pures et appliquées*, 3e série, tome 3 (1877), 219-306.

[2] A. Leissa, The free vibration of rectangular plates, *Journal of Sound and Vibration*, 31 (1973), 257-293.

[3] W. Voigt, Observations on the problem of the transverse vibrations of rectangular plates (in German), *Nachr. Ges. Wiss. (Gottingen)*, 6 (1893), 225-230.

[4] J.N. Reddy, *Theory and Analysis of Elastic Plates and Shells*, 2nd ed., CRC Press, Boca Raton, FL, 2007.

[5] R. Szilard, *Theories and Applications of Plate Analysis: Classical, Numerical and Engineering Methods*, John Wiley & Sons, 2004.

[6] S.H. Hashemi, M. Arsanjani, Exact characteristic equations for some of classical boundary conditions of vibrating moderately thick rectangular plates, *International Journal of Solids and Structures*, 42 (2005), 819-853.

[7] Y. Xiang, Y.B. Zhao, G.W. Wei, Levy solutions for vibration of multi-span rectangular plates, *International Journal of Mechanical Sciences*, 44 (2002), 1195-1218.

[8] Y. Xiang, G.W. Wei, Exact solutions for vibration of multi-span rectangular Mindlin plates, *Journal of Vibration and Acoustics*, 124 (2002), 545-551.

[9] Y. Xiang, C.M. Wang, Exact buckling and vibration solutions for stepped rectangular plates, *Journal of Sound and Vibration*, 250 (2002), 503-517.

[10] Y. Xiang, G.W. Wei, Exact solutions for buckling and vibration of stepped rectangular Mindlin plates, *International Journal of Solids and Structures*, 41 (2004), 279-294.

[11] S.H. Hashemi, M. Fadaee, H.R.D. Taher, Exact solutions for free flexural vibration of Levy-type rectangular thick plates via third-order shear deformation theory, *Applied Mathematical Modelling*, 35 (2011), 708-727.

[12] J.N. Reddy, A.A. Khdeir, L. Librescu, Levy type solutions for symmetrically laminated rectangular plates using first-order shear deformation theory, *Journal of Applied Mechanics*, 54 (1987), 740-742.

[13] A.A. Khdeir, J.N. Reddy, L. Librescu, Analytical solution of a refined shear deformation theory for rectangular composite plates, *International Journal of Solids and Structures*, 23 (1987), 1447-1463.

[14] L. Librescu, A.A. Khdeir, Analysis of symmetric cross-ply laminated elastic plates using a higher-order theory: Part I - Stress and displacement, *Composite Structures*, 9 (1988), 189-213.

[15] A.A. Khdeir, L. Librescu, Analysis of symmetric cross-ply laminated elastic plates using a higher-order theory: Part II - Buckling and free vibration, *Composite Structures*, 9 (1988), 259-277.

[16] A.A. Khdeir, Free vibration of antisymmetric angle-ply laminated plates including various boundary conditions, *Journal of Sound and Vibration*, 122 (1988), 377-388.

[17] A.A. Khdeir, Free vibration and buckling of symmetric cross-ply laminated plates by an exact method, *Journal of Sound and Vibration*, 126 (1988), 447-461.

[18] A.A. Khdeir, J.N. Reddy, Free vibrations of laminated composite plates using second-order shear deformation theory, *Computers and Structures*, 71 (1999), 617-626.

[19] H.-T. Thai, S.-E. Kim, Levy-type solution for free vibration analysis of orthotropic plates based on two variable refined plate theory, *Applied Mathematical Modelling*, 36 (2012), 3870-3882.

[20] A. Hasani Baferani, A.R. Saidi, E. Jomehzadeh, An exact solution for free vibration of thin functionally graded rectangular plates, *Proceedings of the Institution of Mechanical Engineers, Part C: Journal of Mechanical Engineering Science*, 225 (2011), 526-536.

[21] Sh. Hosseini-Hashemi, M. Fadaee, S.R. Atashipour, A new exact analytical approach for free vibration of Reissner-Mindlin functionally graded rectangular plates, *International Journal of Mechanical Sciences*, 53 (2011), 11-22.

[22] Sh. Hosseini-Hashemi, M. Fadaee, S.R. Atashipour, Study on the free vibration of thick functionally graded rectangular plates according to a new exact closed-form procedure, *Composite Structures*, 93 (2011), 722-735.

[23] A. Hasani Baferani, A.R. Saidi, H. Ehteshami, Accurate solution for free vibration analysis of functionally graded thick rectangular plates resting on elastic foundation, *Composite Structures*, 93 (2011), 1842-1853.

[24] L.W. Zhang, Z.G. Song, K.M. Liew, State-space Levy method for vibration analysis of FG-CNT composite plates subjected to in-plane loads based on higher-order shear deformation theory, *Composite Structures*, 134 (2015), 989-1003.

[25] A.A. Khdeir, J.N. Reddy, Influence of edge conditions on the modal characteristics of cross-ply laminated shells, *Computers & Structures*, 34 (1990), 817-826.

[26] Sh. Hosseini-Hashemi, M.R. Ilkhani, M. Fadaee, Identification of the validity range of Donnell and Sanders shell theories using an exact vibration analysis of functionally graded thick cylindrical shell panel, *Acta Mechanica*, 223 (2012), 1101-1118.

[27] Sh. Hosseini-Hashemi, M. Fadaee, On the free vibration of moderately thick spherical shell panel?A new exact closed-form procedure, *Journal of Sound and Vibration*, 330 (2011), 4352-4367.

[28] Sh. Hosseini-Hashemi, S. R. Atashipour, M. Fadaee, U. A. Girhammar, An exact closed-form procedure for free vibration analysis of laminated spherical shell panels based on Sanders theory, *Archive of Applied Mechanics*, 82 (2012), 985-1002.

[29] A refined dynamic stiffness element for free vibration analysis of cross-ply laminated composite cylindrical and spherical shallow shells, *Composites Part B: Engineering*, 62 (2014), 143-158.

[30] E. Carrera, Theories and finite elements for multilayered, anisotropic, composite plates and shells, *Archives of Computational Methods in Engineering*, 9 (2002), 87-140.

[31] L. Dozio, Exact vibration solutions for cross-ply laminated plates with two opposite edges simply supported using refined theories of variable order, *Journal of Sound and Vibration*, 333 (2014), 2347-2359.

[32] L. Dozio, Exact free vibration analysis of Levy FGM plates with higher-order shear and normal deformation theories, *Composite Structures*, 111 (2014), 415-425.

[33] A.S. Rezaei, A.R. Saidi, Application of Carrera Unified Formulation to study the effect of porosity on natural frequencies of thick porous-cellular plates, *Composites Part B: Engineering*, 2016, in press.

[34] A.H. Mohazzab, L. Dozio, Prediction of natural frequencies of laminated curved panels using refined 2-D theories in the spectral collocation method, *Curved and Layered Structures*, 2 (2015), 1-14.

[35] F. Tornabene, S. Brischetto, N. Fantuzzi, E. Viola, Numerical and exact models for free vibration analysis of cylindrical and spherical shell panels, *Composites Part B: Engineering*, 81 (2015), 231-250.

[36] J.N. Reddy, *Mechanics of Laminated Composite Plates and Shells: Theory and Analysis*, CRC Press, Boca Raton, FL, 2004.

[37] S. Brischetto, Three-Dimensional Exact Free Vibration Analysis of Spherical, Cylindrical, and Flat One-Layered Panels, *Shock and Vibration*, Volume 2014, Article ID 479738, 29 pages.

[38] S. Brischetto, An Exact 3D Solution for Free Vibrations of Multilayered Cross-Ply Composite and Sandwich Plates and Shells, *International Journal of Applied Mechanics*, 6 (2014), Article ID 1450076, 42 pages.